Supporting Information

A pyrene-based electropolymerized film as a solid-state platform for multi-bit memory storage and fluorescent sensing of nitroaromatics in aqueous solutions

Megha Chhatwal, Anup Kumar, Rinkoo D. Gupta, Satish K. Awasthi**

Megha Chhatwal, Anup Kumar, Prof. Satish. K. Awasthi
Chemical Biology Laboratory, Department of Chemistry, University of Delhi, Delhi-110 007, India.
E-mail: skawasthi@chemistry.du.ac.in

Dr. Rinkoo D. Gupta
Faculty of Life Sciences and Biotechnology, South Asian University, New Delhi-110 021, India

Materials and methods: The chemicals *viz.* 2-acetyl pyridine, $(NH_4)_2OsCl_6$ and NH_4PF_6 were purchased from Sigma Aldrich and used without further purification. 1-Pyrenecarboxaldehyde was bought from Alfa Aesar. Solvents (HPLC grade) were purchased from Merck and distilled using reported methods.[S1] Picric acid, 1-chloro 2,4-dinitrobenzene, nitrobenzene and all other quenchers like benzonitrile, benzoquinone, benzoic acid, toluene, benzene and aniline were purchased from s. d. fine and Rankem Chemicals Pvt. Ltd. Indium-tin-oxide coated glass was purchased from Scientific Technologies (India). Deuterated solvents ($CDCl_3$ and CD_3CN) were purchased from Sigma Aldrich and stored under freezer. The ^{1}H-NMR spectrum was recorded at room temperature using Jeol JNMECX 400P spectrometer. All chemical shifts (δ) were recorded in ppm with reference to tetramethylsilane and coupling constant (J) have been reported in Hz. Mass spectra were recorded on a mass spectrometer by Agilent Technology, USIC, University of Delhi, India.

Characterization of Os(pyrtpy)$_2$.2PF$_6$, ***1****:* 9.11 (s, 4H, $H^{3',5',tpy}$), 8.74 (d, J = 9.2 Hz, 2H, $H^{2,pyrene}$), 8.61-8.56 (m, 6H, $H^{3,3'',tpy}$+$H^{10,pyrene}$), 8.47 (d, J = 7.8 Hz, 2H, $H^{3,pyrene}$), 8.43-8.34 (m, 10H, pyrenyl protons), 8.2 (t, J = 7.6 Hz, 2H, $H^{7,pyrene}$), 7.82 (td, J = 7.8, 1.3 Hz, 4H, $H^{4,4'',tpy}$), 7.53 (d, J = 6.0 Hz, 4H, $H^{6,6'',tpy}$), 7.29 (td, J = 6.5, 1.2 Hz, 4H, $H^{5,5'',tpy}$); ESI-MS (calculated for $C_{62}H_{38}F_{12}N_6P_2Os$) m/z = 528.79 $[M\text{-}2PF_6^-]^{2+}$, 1056.34 $[M\text{-}2PF_6^-\text{-}H^+]^+$, UV–vis (~ 10^{-5} M, CH_3CN): λ (nm) (ε, M^{-1} cm^{-1}) = 238 (1,31,700), 275 (92,000), 313 (83,000), 491 (35,000), 667 (8,000); CV (~ 10^{-4} M *vs.* Ag/AgCl, 0.1 M TBAP, CH_3CN): $E_{1/2}$ ($Os^{2+/3+}$) = 1.05 V, E_{oxd} (pyrene) = ~+1.48 V.

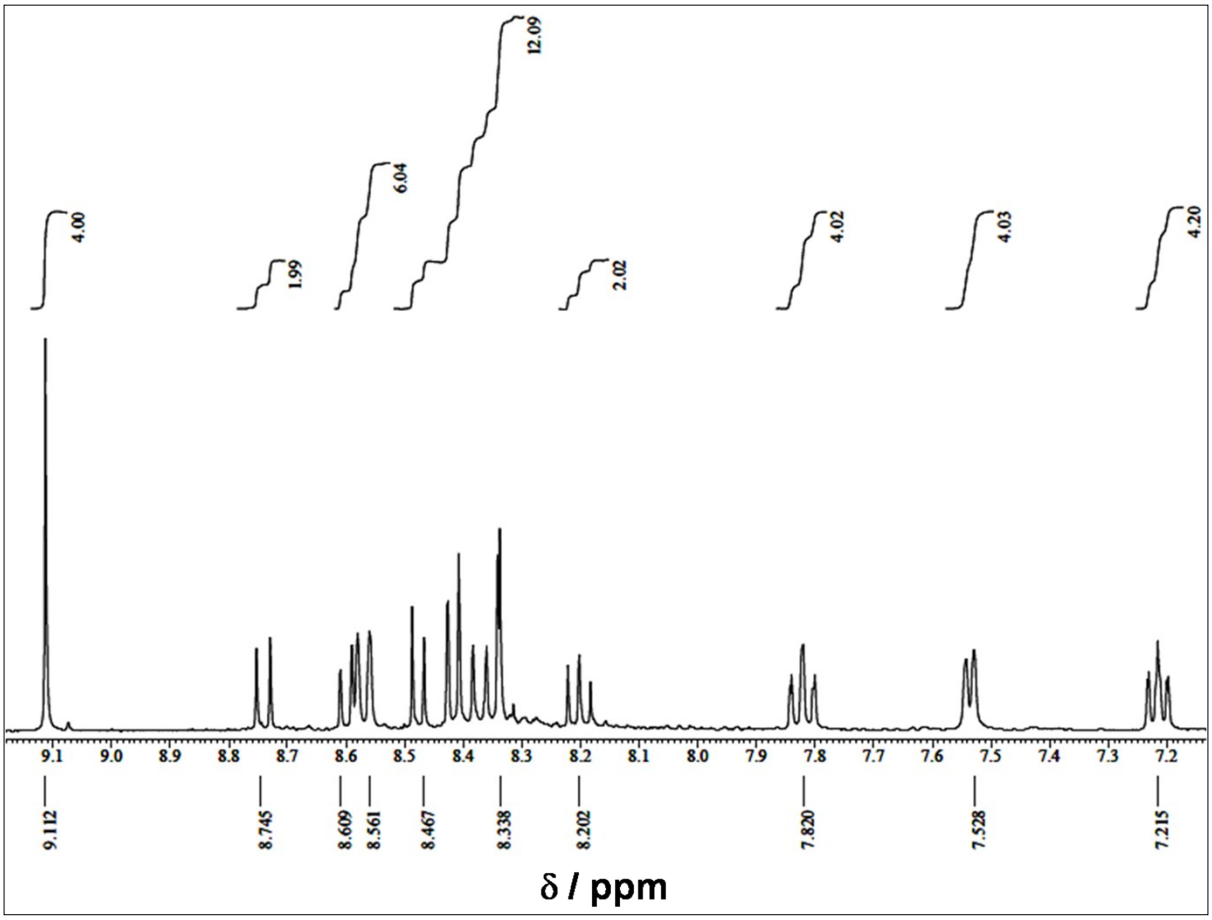

Figure S1. ^{1}H-NMR spectrum of complex **1** in CD_3CN

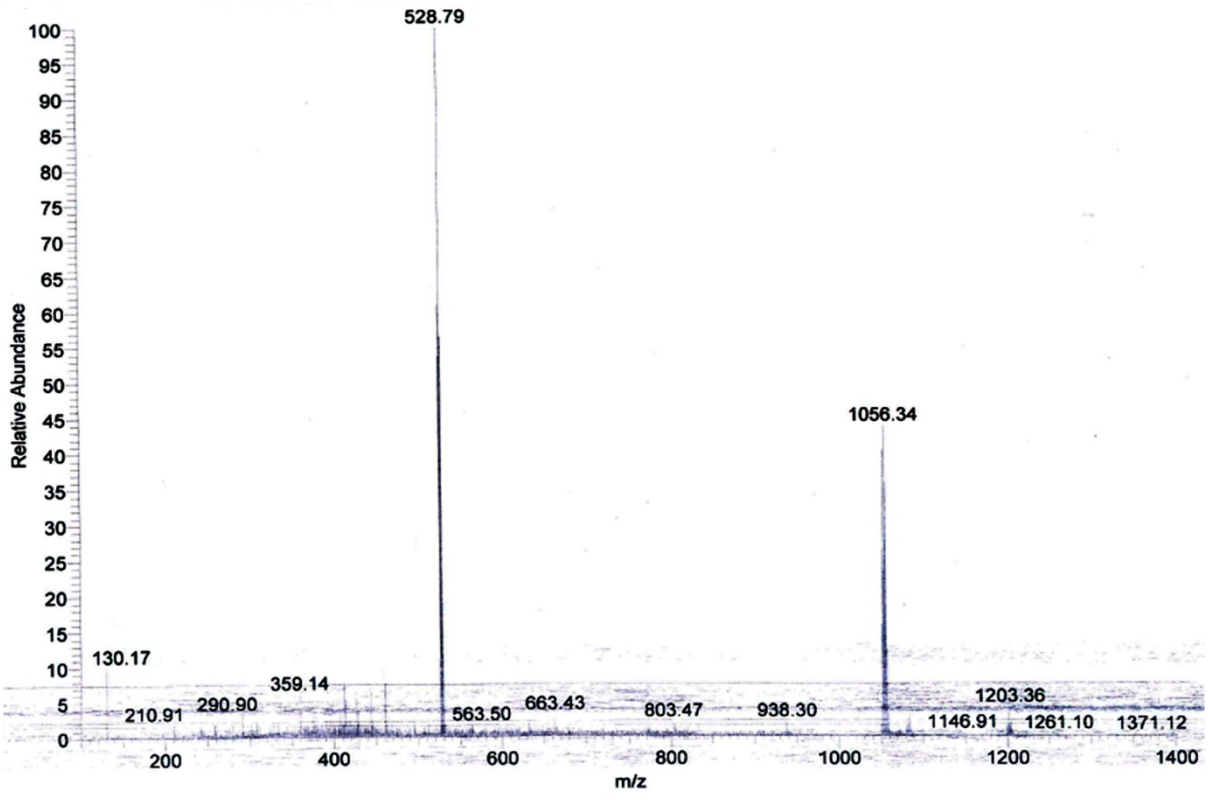

Figure S2. ESI-MS of complex **1**

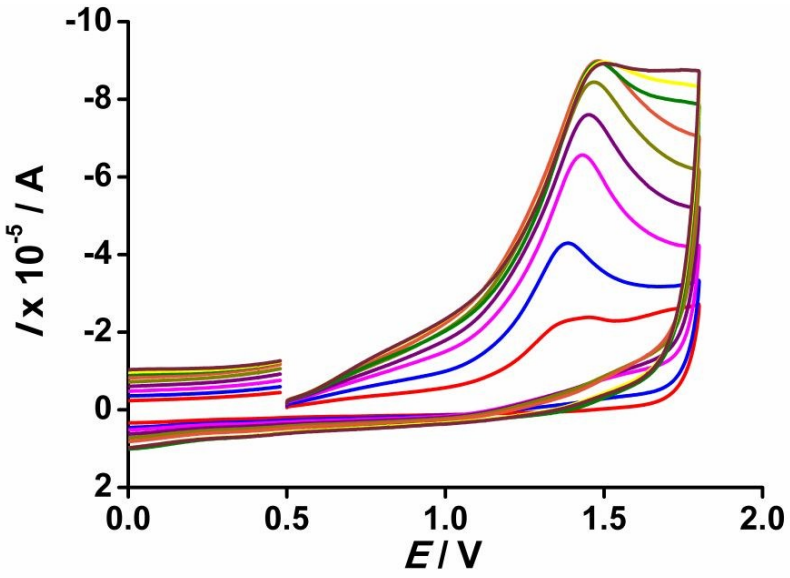

Figure S3. Cyclic voltammogram of pyrtpy ligand (~10^{-3} M, *vs.* Ag/AgCl, 0.1 M Bu_4NPF_6, CH_3CN) at scan rates ranging from 0.1 to 1.0 Vs^{-1}.

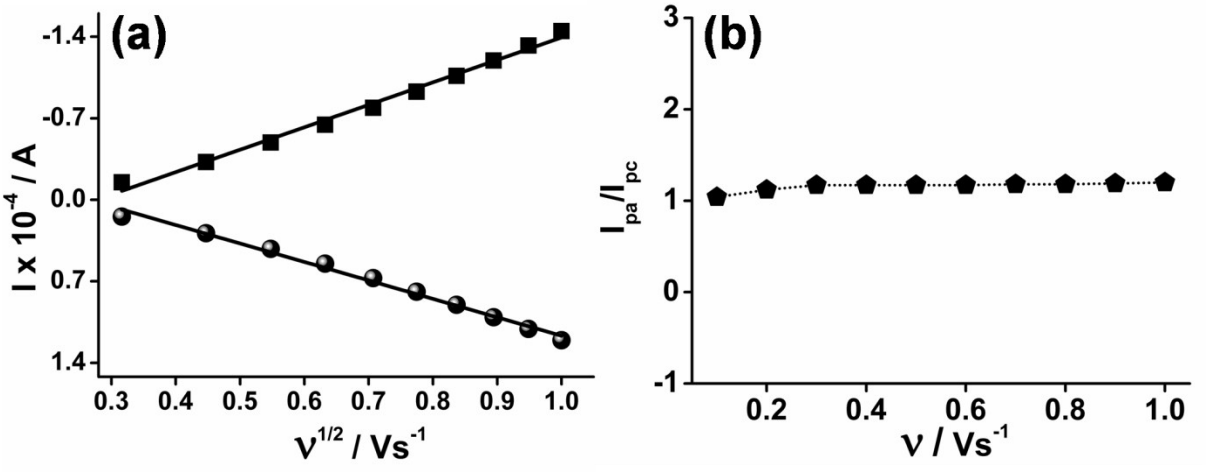

Figure S4. (a) Linear dependence of anodic (squares) and cathodic (spheres) peak currents of **complex 1** on scan rate ($R^2 = 0.99$), (b) Plot of anodic and cathodic peak current ratio (I_{pa}/I_{pc}) as a function of scan rate.

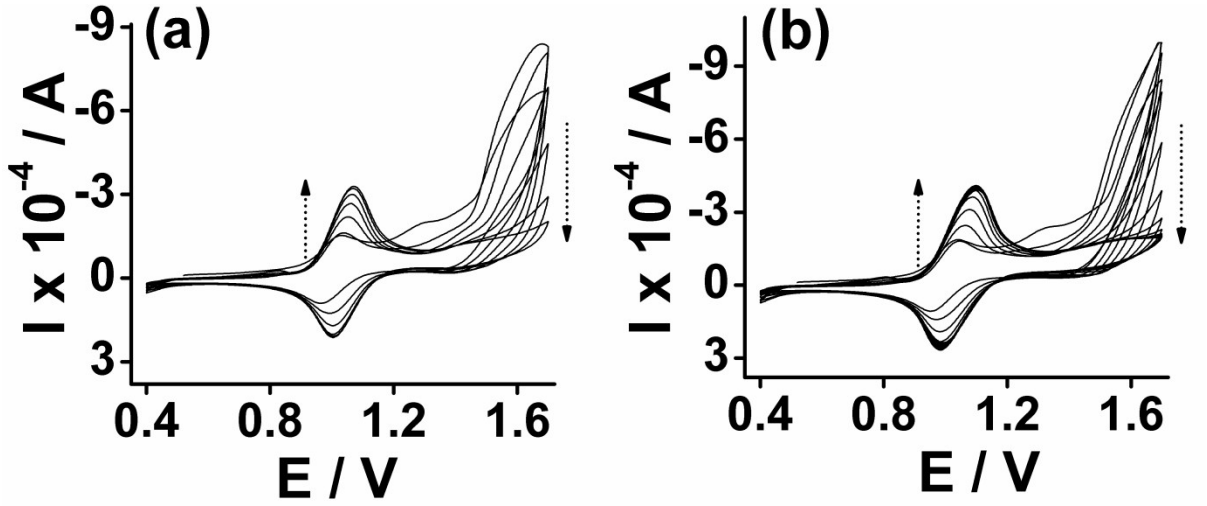

Figure S5. Oxidative electropolymerization of **1** (~0.5 × 10^{-3} M, *vs.* Ag/AgCl, 0.1 M Bu_4NPF_6, CH_3CN) on ITO electrode by (a) 5 and (b) 10 successive potential scans at 50 mVs^{-1}.

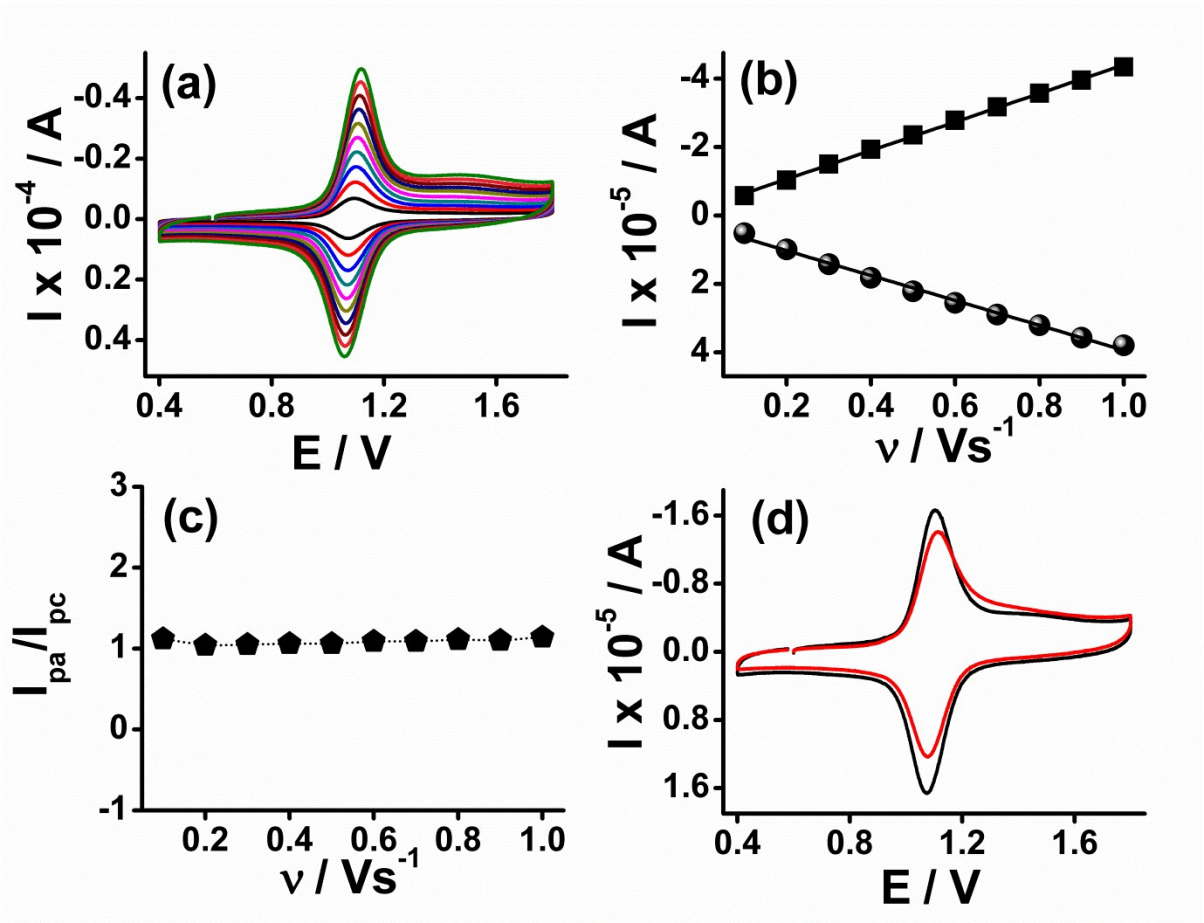

Figure S6. (a) Cyclic voltammetric profiles of **1-GCE** polymeric film (surface coverage = ~4.8 × 10^{-10} mol cm^{-2}) at scan rates ranging from 0.1 to 1 Vs^{-1}, (b) Linear dependence of anodic (squares) and cathodic (spheres) peak currents of the film on scan rate (R^2 = 0.99), (c) Plot of anodic and cathodic peak current ratio (I_{pa}/I_{pc}) as a function of scan rate, (d) Cyclic voltammetric profiles of the film before (black line) and after (red line) 3 × 10^2 cycles of potential stress at the scan rate 0.3 Vs^{-1}.

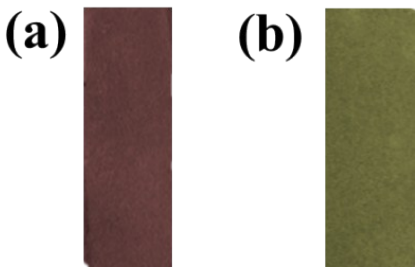

Figure S7. Visual colour change of **1-ITO** polymeric film a) before and b) after oxidation by applying potential of +1.25 V.

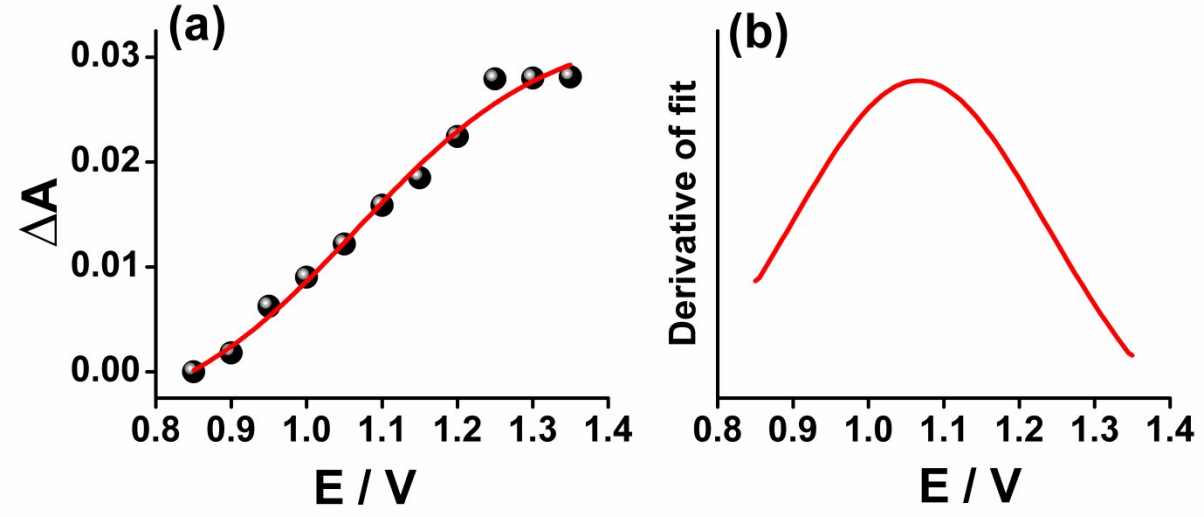

Figure S8. (a) Optical response of **1-ITO** film at the ^{1}MLCT band (λ = 500 nm) as a function of voltage upon applying double-potential steps between +0.85 V and (0.85 V + n0.05 V); n = 1, 2.....10 with 20 s interval. Each data point represents the average of 10 double-potential cycles. The red line depicts the sigmoidal fit of the data (R^2 = 0.98) with an inflection point at 1.06 V, (b) Derivative of the sigmoidal fit with full-width at half-maximum (FWHM) value of 0.40 V.

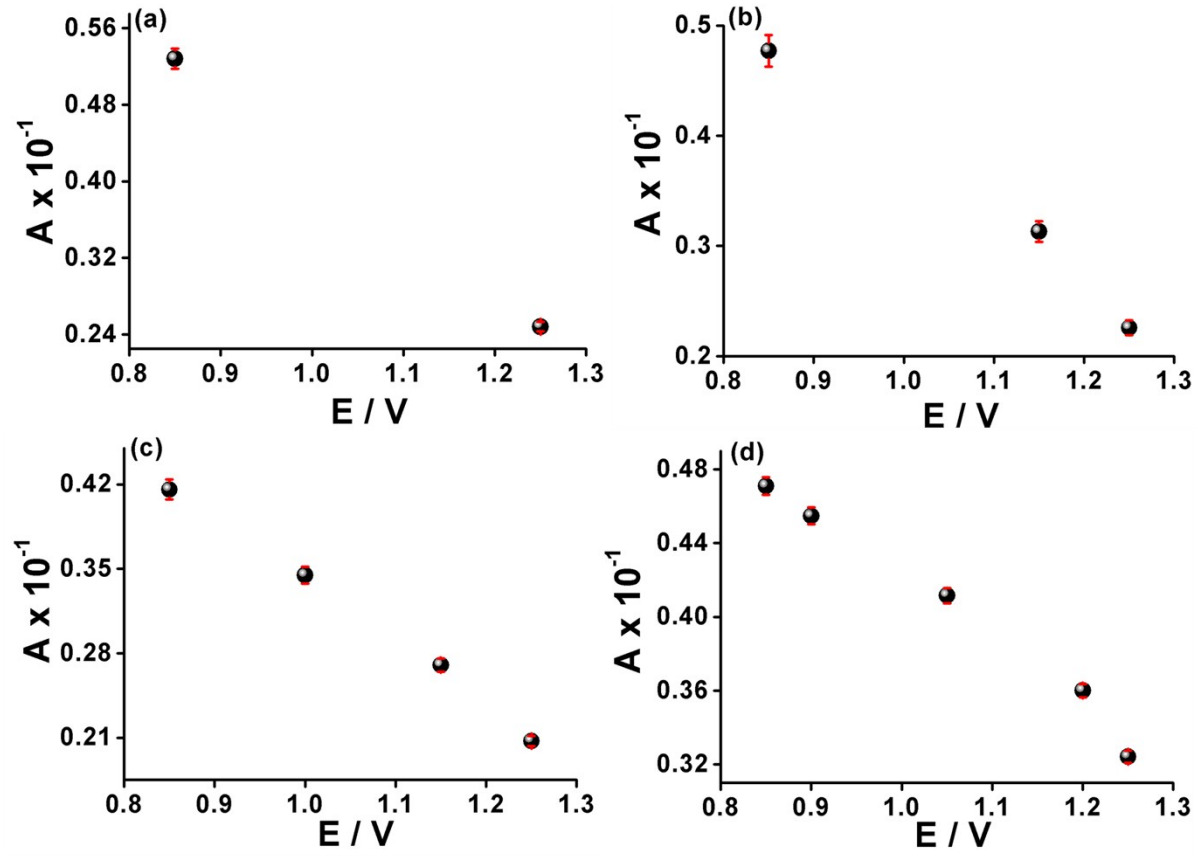

Figure S9. (a) Double-potential step, (b) Triple-potential step, (c) Quadruple-potential step and (d) Quintuple potential step switching of **1-ITO** polymeric film at ^{1}MLCT band using same set-up for three experiments.

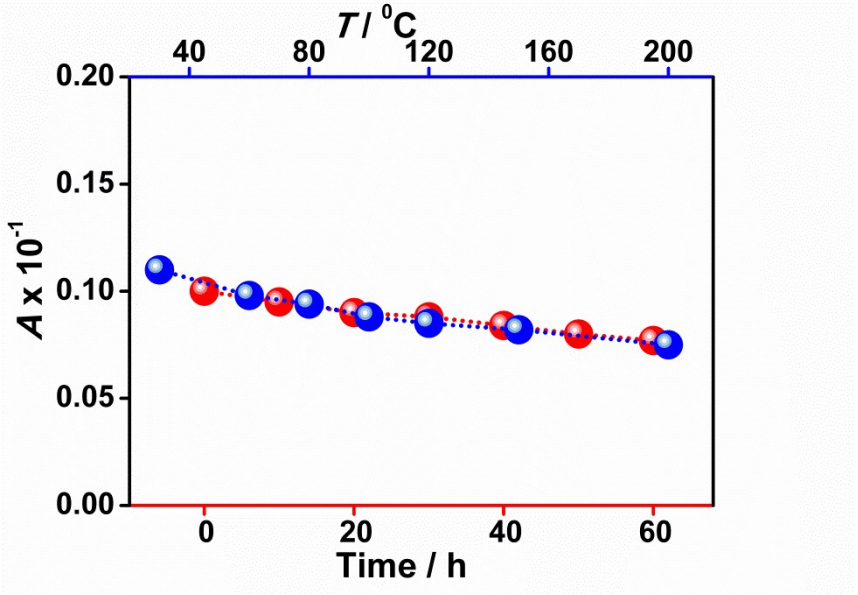

Figure S10. UV-vis monitoring of thermal (blue spheres, for ~ 1 h) and temporal (red spheres, at 200°C) stability of **1-ITO** polymeric film.

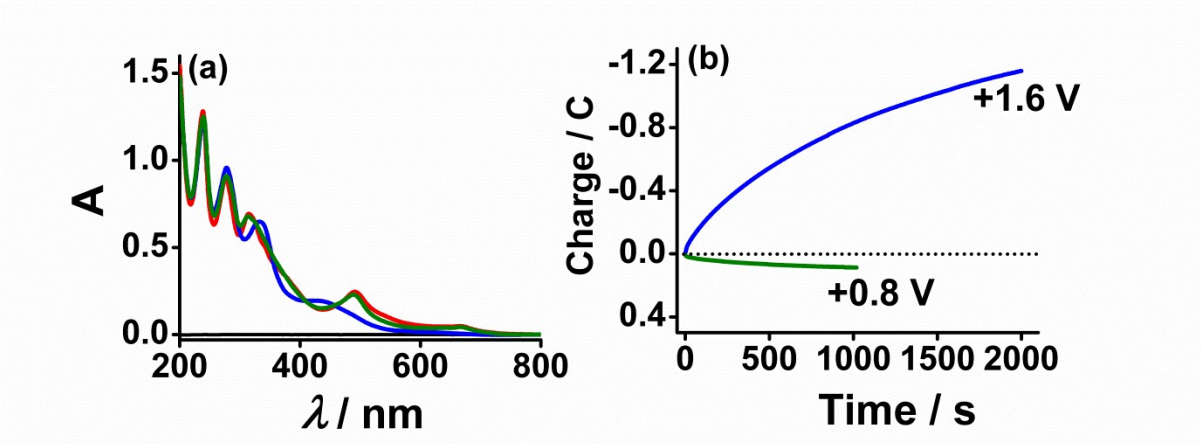

Figure S11. (a) Absorbance changes in **complex 1** (~0.7 × 10^{-5} M, *vs.* Ag/AgCl, 20 mM Bu_4NPF_6, CH_3CN, red solid line) upon applying voltage input for oxidation at +1.6 V (blue solid line) and reduction at +0.8 V (green solid line), (b) Plot of charge *vs.* time, for oxidation (blue trace) and reduction (green trace) of osmium centers at suitable potential.

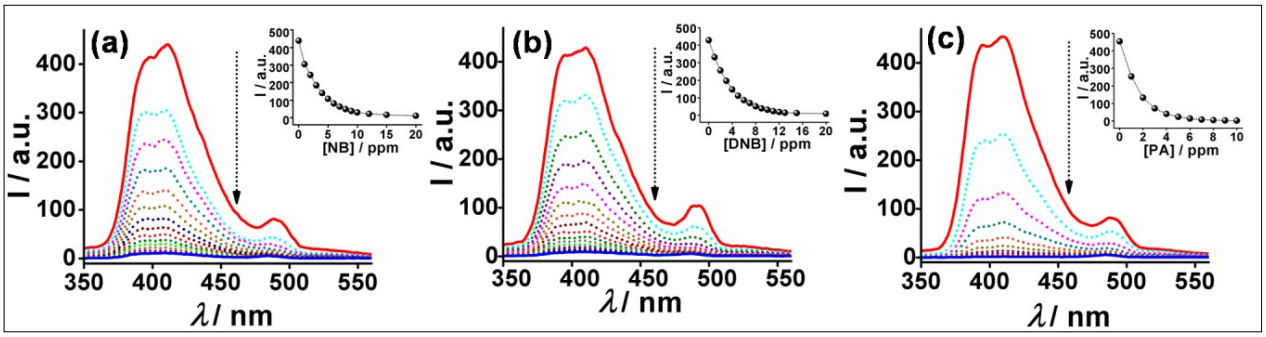

Figure S12: Emission intensity changes in **complex 1** (10^{-5} M, CH_3CN) upon addition of (a) 0-20 ppm of NB, (b) 0-20 ppm of DNB and (c) 0-10 ppm of PA in CH_3CN. The excitation wavelength was fixed at λ = 238 nm. The dotted arrows serve guide to the eyes. Insets: Plots of emission intensity at λ = 410 nm as a function of ppm concentration of NACs.

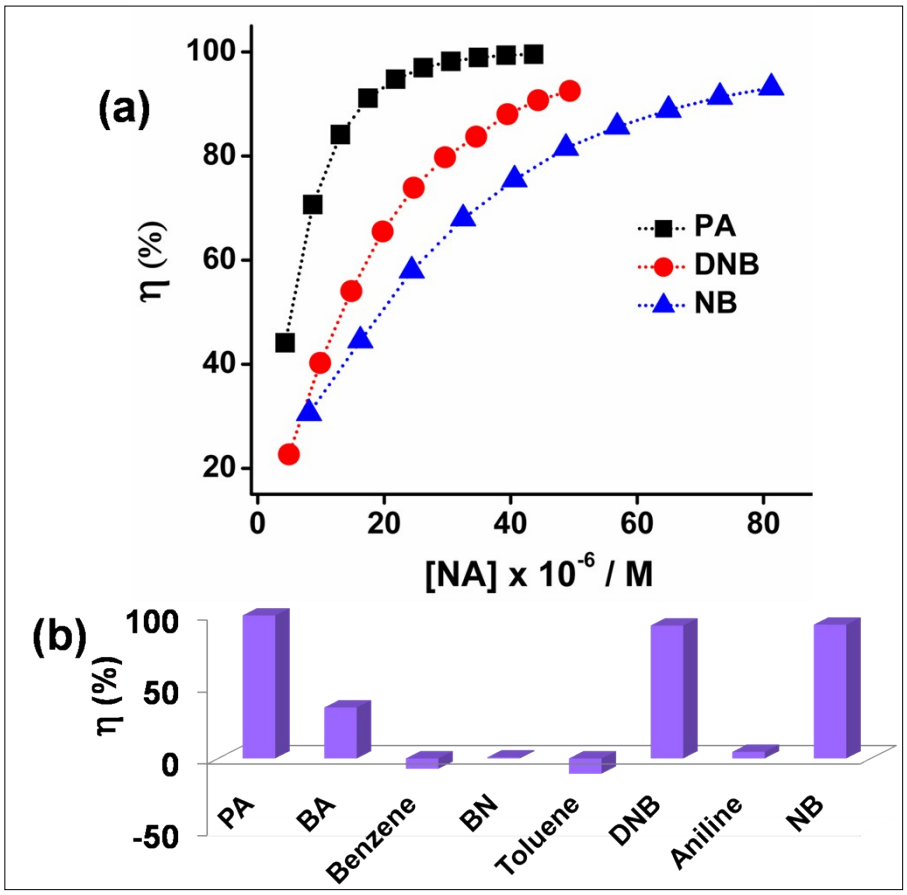

Figure S13: (a) Quenching efficiency (η%) of **complex 1** (10^{-5} M, CH_3CN) for different NACs at λ = 410 nm, (b) Representative bar chart showing selective sensing by **complex 1** (10^{-5} M, CH_3CN)at λ = 410 nm upon addition of various competitive quenchers (20 ppm, CH_3CN). PA: picric acid, BA: benzoic acid, BN: benzonitrile, DNB: 1-chloro 2,4-dinitrobenzene and NB: nitrobenzene.

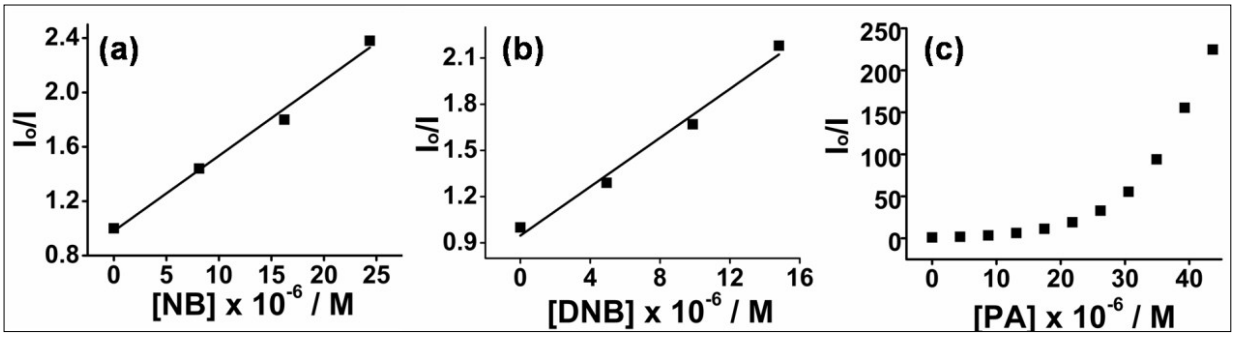

Figure S14: Stern-Volmer plots for the fluorescence quenching of **complex 1** (10^{-5} M, CH_3CN) at $\lambda = 410$ nm by (a) NB, (b) DNB and (c) PA. The linear fit has the R^2 value of 0.97-0.98.

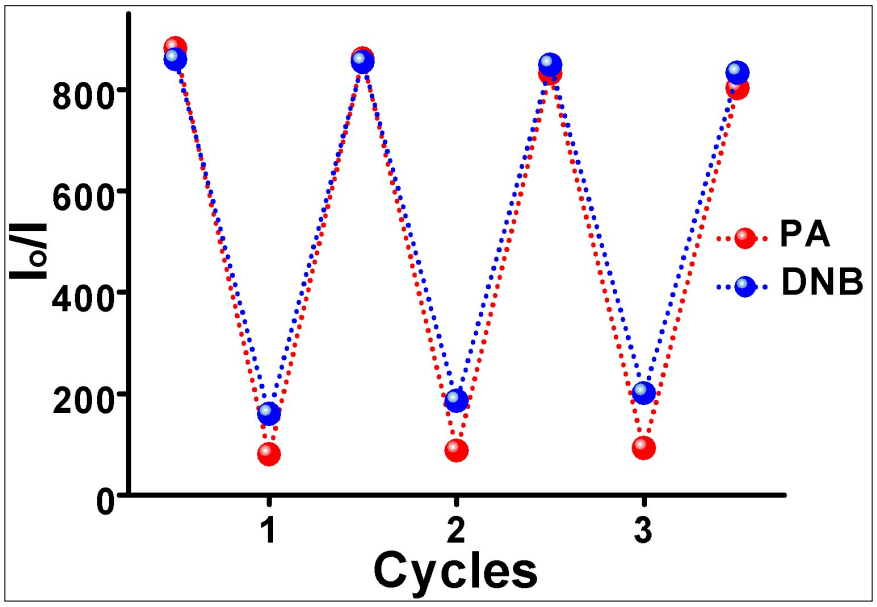

Figure S15: The sensing-recovery cycles for **1-ITO** film upon addition of PA (50 ppm, red spheres) and DNB (15 ppm, blue spheres) and subsequent regeneration of emission in water. Dotted lines serve guide to eyes.

References:

S1: D. D. Perrin and W. L. F. Armarego, *Purification of Laboratory Chemicals*, 3. Aufl., Oxford. Pergamon Press, **1988**.

S2: X.-G. Li, Y.-W. Liu, M.-R. Huang, S. Peng, L.-Z. Gong, M. G. Moloney, *Chem. Eur. J.* **2010**, *16*, 4803.